An investigation of leaf-blade anatomy and photosynthetic characteristics of four Cyperaceae species from the Albany and Bathurst districts in the eastern Cape

B.J. Sonnenberg and C.E.J. Botha*

Department of Botany, Schönland Laboratories, Rhodes University, P.O. Box 94, Grahamstown, 6140 Republic of South Africa

Received 17 July 1991; revised 13 May 1992

The anatomy of the leaf-blades of four field-grown Cyperaceae, namely *Cyperus albostriatus* Schrad., *Cyperus fastigiatus* Rottb., *Cyperus pulcher* Thunb. and *Mariscus congestus* (Vahl.) C.B.Cl., was investigated with light and scanning electron microscopes, to determine stomatal type and frequencies. Photosynthetic characteristics, including light and temperature response as well as post-illumination CO_2 burst effect, were investigated using an ADC 225 MKIII infra-red gas analyser in open circuit. The leaf anatomy and gas exchange response suggest that *C. pulcher* is a C_3 species, whilst *C. albostriatus, C. fastigiatus* and *M. congestus* are C_4. The post-illumination CO_2 burst studies suggest that *C. albostriatus* and *M. congestus* are C_4-NADP-Me species type and that *C. fastigiatus* is either NAD-Me or PCK.

Die anatomie van die blaarskywe van vier Cyperaceae spesies wat natuurlik voorkom, naamlik *Cyperus albostriatus* Schrad., *Cyperus fastigiatus* Rottb., *Cyperus pulcher* Thunb. en *Mariscus congestus* (Vahl.) C.B.Cl., is met behulp van lig- en skandeermikroskope ondersoek om die aantal en tipe huidmondjies vas te stel. Fotosintetiese eienskappe, insluitende reaksie op lig en temperatuur sowel as die skielike verhoging van vrygestelde CO_2 na beligting, is met behulp van 'n ADC 225 MKIII infrarooi-gasontleder, gekoppel in 'n oop stroomkring, ondersoek. Die blaar-anatomie en gaswisselingsreaksie dui daarop dat *C. pulcher* 'n C_3 spesie is terwyl *C. albostriatus, C. fastigiatus* en *M. congestus* almal C_4 spesies is. Die studie van die verhoging van CO_2 na beligting dui daarop dat *C. albostriatus* en *M. congestus* C_4-NADP-Me spesies is en dat *C. fastigiatus* 'n MAD-Me of PCK spesie is.

Keywords: Cyperaceae, infra-red gas analysis, leaf anatomy, photosynthesis.

*To whom correspondence should be addressed.

Introduction

The anatomy of northern hemisphere Cyperaceae has been studied thoroughly by several researchers (Plowman 1906; Pfeiffer 1927; Metcalfe 1969; Brown 1975; Carolin *et al.* 1977). However, few photosynthetic gas exchange investigations of Cyperaceae have been undertaken and research has involved enzyme assay (Ueno *et al.* 1986; Bruhl *et al.* 1987) or carbon isotope ratios (Hesla *et al.* 1982; Ueno *et al.* 1989).

Previous anatomical studies have shown that both C_3 and C_4 photosynthetic forms exist in the Cyperaceae. In the Cyperaceae, the Kranz mesophyll, or primary carbon assimilation (PCA) cells, are separated from the primary carbon reduction cells (PCR) or bundle sheath cells, by a layer of cells which has been termed the mestome sheath (Metcalfe 1969; Laetsch 1974; Brown 1975; Carolin *et al.* 1977). Members of the Cyperaceae may be separated anatomically into fimbristylloid, chlorocyperiod (Raynal 1973; Brown 1975; Takeda *et al.* 1985) and the recently-described rhynchosporoid (Takeda *et al.* 1980) types.

Until recently it was believed that all C_4 Cyperaceae species were NADP-Me (Metcalfe 1969; Ueno 1986). All previous photosynthetic investigations seem to support this (Carolin *et al.* 1977; Ueno *et al.* 1986). However, several records of NAD-Me Cyperaceae, namely *Eleocharis vivipara, E. caespitasissima* and *E. retroflexan*, have been reported by Bruhl *et al.* (1987) and Ueno *et al.* (1988).

Materials and Methods

Plant material

Plant material was collected from the Albany and Bathurst districts. Specifically, *Cyperus albostriatus* Schrad. from Dasie Krans (*Sonnenberg 70*, RUH), *Cyperus fastigiatus* Rottb. from the river banks of the Lushington River near Bathurst (*Sonnenberg 160*, RUH), *Cyperus pulcher* Thunb. from the Blaauwkrans Mountain Reserve (*Sonnenberg 134*, RUH) and *Mariscus congestus* (Vahl.) C.B.Cl. from the forested region of Dasie Krans (*Sonnenberg 78*, RUH). All voucher specimens are housed in the Rhodes University Herbarium.

Specimens were collected and potted in a mixture of potting soil and river sand (1:3 w/w ratio). The potted specimens were left for a period of two weeks prior to conducting gas exchange experiments.

Anatomical studies

Light microscopy

Portions of mature leaf material (10 mm × 10 mm) were excised from the mid-laminar regions of the leaves of each species and fixed in formyl acetic acid (FAA). Thereafter, segments were sequentially dehydrated in an ethanol and tertiary butyl alcohol series and subsequently infiltrated with paraplast, blocked and sectioned using a Leitz Wetzlar 1212 rotary microtome (Leitz, Johannesburg) at 10 μm. Serial sections were mounted on slides and stained in safranin and

fast green cfc. Selected sections were viewed and photographed using a Zeiss microscope fitted with an MC-63 camera (Carl Zeiss Pty Ltd, Johannesburg) using Agfapan 25 film (Agfa Pty Ltd, Johannesburg).

Scanning electron microscopy

Segments of mature mid-laminar leaf material (10 mm × 5 mm) were excised from each species and fixed in 2.5% glutaraldehyde in 0.1 M phosphate buffer (pH 7.3) at 4°C, with two fixative changes within a 24-h period. Sections were subsequently dehydrated in an ethanol/amyl acetate series and critical-point-dried. Two specimens of each species were mounted on brass stubs, such that both the adaxial and abaxial surfaces could be compared and photographed on the same stub. Each stub was sputter-coated with gold, viewed and photographed at magnifications of 10 000 and 1000× using a Jeol SM 830 scanning electron microscope (Jeol, Tokyo, Japan) at 20 kV.

Gas exchange experiments

The investigation of photosynthetic characteristics was carried out using a calibrated ADC 225 MKIII infra-red gas analyser (ADC, Hoddesdon, England) in open circuit and in differential mode. A Vialux NAV-T 400-W high-pressure sodium lamp (S.A. Phillips, Port Elizabeth, South Africa) was used as a light source. An MGW-RC 6 Lauda (Optolabor, Johannesburg) was coupled to water-jacketed cuvettes, to control the experiments. The photon flux density (μmol m^{-2} s^{-1}), temperature, CO_2 differential and leaf area in each cuvette were recorded and the net assimilation rates (A) were calculated as μmol CO_2 m^{-2} s^{-1}. Each experiment was conducted in triplicate and repeated twice, using mature leaves. Graphic data presented are means of all experiments for the different plants.

Light and temperature response experiments

The light response of each species was investigated at constant temperature using the previously described temperature-controlled cuvettes. Shade cloth of differing thicknesses was used to vary the light intensity. Maximum photosynthetic rate (A_{max}) was determined for each species, at varying light and temperature levels. The light response of each species was determined at the following photosynthetic photon flux densities: 0, 12.5, 25, 50, 75, 125, 250, 500, 750, 1000, 1400 and 2000 μmol m^{-2} s^{-1}. The temperature response for each species was determined at 15, 20, 25, 30, 35 and 40°C.

Post-illumination CO_2 burst effect (PIB)

Attached leaves of each species were sealed into cuvettes, at their respective optimal temperature and at a light intensity of 1500 μmol m^{-2} s^{-1}. Once the leaves had attained maximal photosynthetic rates, the light source was switched off and the cuvette immediately covered in black plastic. The response of leaves to the ensuing darkness was monitored continuously until the leaves attained steady-state net respiration.

Results

Brief description of the anatomy of the leaf blade vascular bundles

Mariscus congestus

The median bundle in *M. congestus* (Figure 1) contains large metaxylem and protoxylem vessels (M and P, respectively, Figure 1). The phloem tissue is surrounded by a ring of parenchymatic cells which contain large chloroplasts. This layer is the functional equivalent to the PCR in this as well as the other C_4 species investigated in this study. The median bundle is in turn, surrounded by a ring of compact, lignified cells which is correctly described as an endodermoid sheath (Johnson & Brown 1973) rather than as a mestome sheath. The outer layer associated with the median bundle consists of a ring of mesophyll cells, which, at the light microscope level, can be seen to contain small chloroplasts. This represents the PCA layer in this and in the other C_4 species investigated. A single hypodermal sclerenchymatous strand occurs adaxially on each side of the median bundle. Small bundles (unlabelled arrows) occur in close proximity to the median bundle. Within the leaf-blade itself (Figure 2), three rows of bundles are discernible — an adaxial row, consisting almost entirely of small bundles (that is, lacking large metaxylem or protoxylem elements), a median row, containing mostly intermediate bundles (that is, containing large metaxylem but no protoxylem elements) and an abaxial row, which, like the adaxial, contains mostly small bundles. All leaf-blade bundles are associated with a loosely-radiate ring of chlorenchymatous cells (the PCA) beneath which is a compact lignified endodermoid sheath, which surrounds a ring of large chloroplast-containing (PCR) cells.

Cyperus albostriatus

Like *M. congestus*, the vascular bundles in the leaf-blades of *C. albostriatus* are arranged in three rows. The adaxial and abaxial rows are composed of small vascular bundles, and a median row that contains intermediate bundles only, which are separated from each other by large air spaces within an essentially aerenchymatous mesophyll (Figures 3 & 4). The spatial relationship of Kranz mesophyll, lignified endodermoid sheath cells and PCR layer are essentially the same as in *C. fastigiatus* and *M. congestus*.

Cyperus fastigiatus

Figure 5 shows the midrib region of a leaf of *C. fastigiatus*. As in the *M. congestus* and *C. albostriatus* leaves, the midrib bundle is associated with lateral hypodermal sclerenchymatous strands (SS, Figure 5). In contrast to *M. congestus* and *C. albostriatus*, the leaf-blade of *C. fastigiatus* contains only two rows of vascular bundles (Figure 6). The adaxial row consists of small and intermediate bundles, whilst the parenchymatous bridge separating the large intercellular spaces (which are formed by stellate parenchyma), is occupied by a large bundle in this instance (Figure 6).

Cyperus pulcher

The deeply-keeled midrib of *C. pulcher* contains a solitary

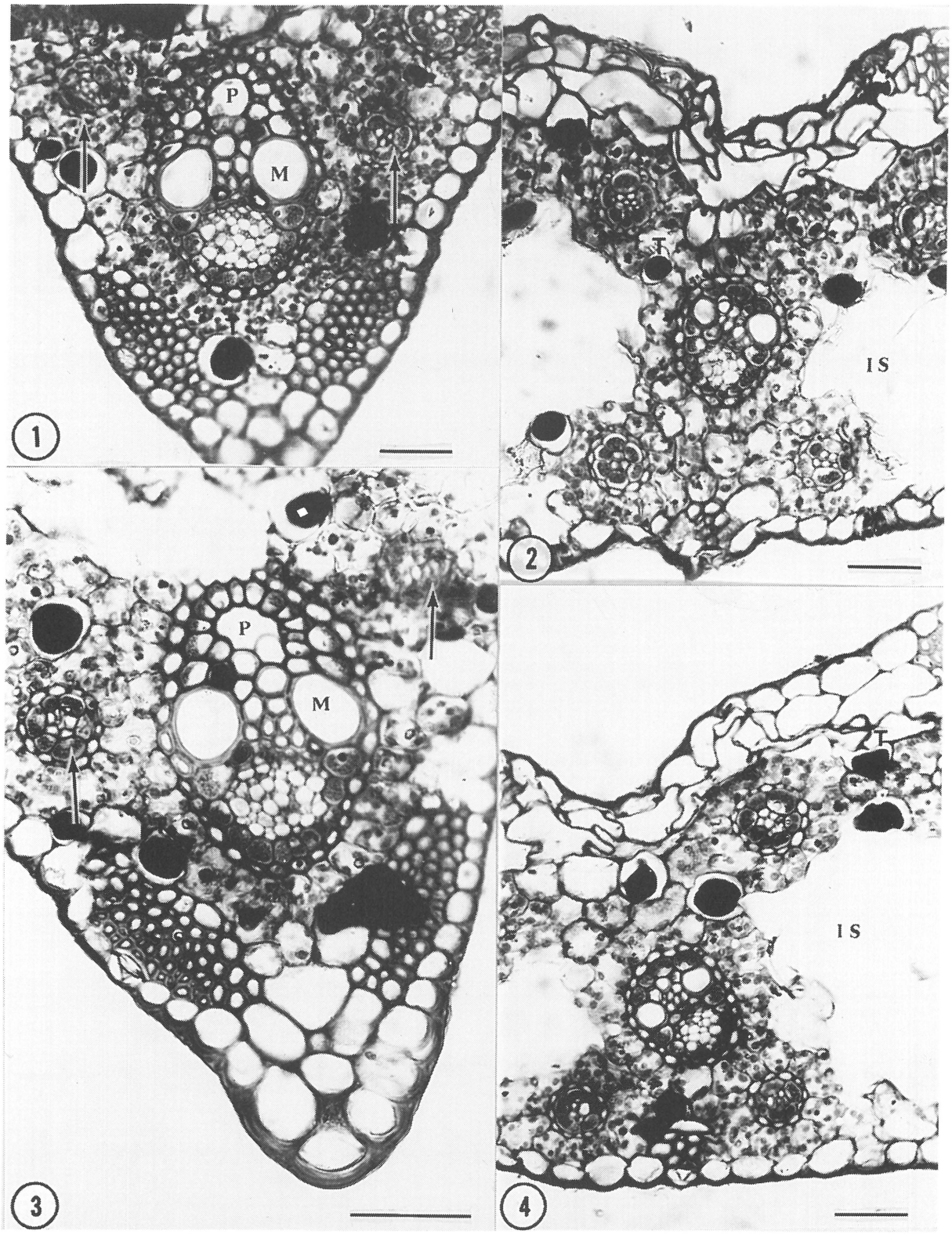

Figures 1, 2 Distribution of vascular bundles in the midrib (Figure 1) and lamina (Figure 2) of *Mariscus congestus*. **1.** An extensive band of sclerenchymatous hypodermal strands (SS) can be seen on either side of the midrib. A compact, thick-walled ring of cells separates the PCA (Kranz) from the PCR (bundle sheath) cells in the midrib. This bundle contains both large metaxylem vessels (M) and a protoxylem (P). **2.** Portion of the lamina of *M. congestus*. The mesophyll contains large intercellular spaces (IS). An intermediate bundle is subtended by the mesophyll bridge between adjacent intercellular spaces. Vascular bundles in this lamina occur in three rows. In both figures, tannin cells (T) occur throughout the lamina. Scale bars: 10μm.

Figures 3, 4 Distributions of vascular bundles in the midrib (Figure 3) and lamina (Figure 4) of *Cyperus albostriatus*. **3.** The PCA is separated from the PCR by a lignified, thickened endodermoid sheath. The midrib bundle contains large metaxylem vessels (M) and a disintegrating protoxylem vessel (P). Sclerenchymatous hypodermal strands (SS) occur on either side of the large midrib vascular bundle. Small bundles (unlabelled arrows), which occur on either side of the midrib bundle, are associated with an endodermoid sheath. **4.** Part of *C. albostriatus* lamina. Large intercellular spaces (IS) occur towards the mid-lamina region and an intermediate bundle is subtended by the mesophyll bridge between adaxial and abaxial small vascular bundles. As in *M. congestus*, small bundles are associated with an endodermoid sheath separating PCA from PCR layers. Tanniniferous cells occur throughout the lamina (T). Scale bars: 20 μm (Figure 3); 10 μm (Figure 4).

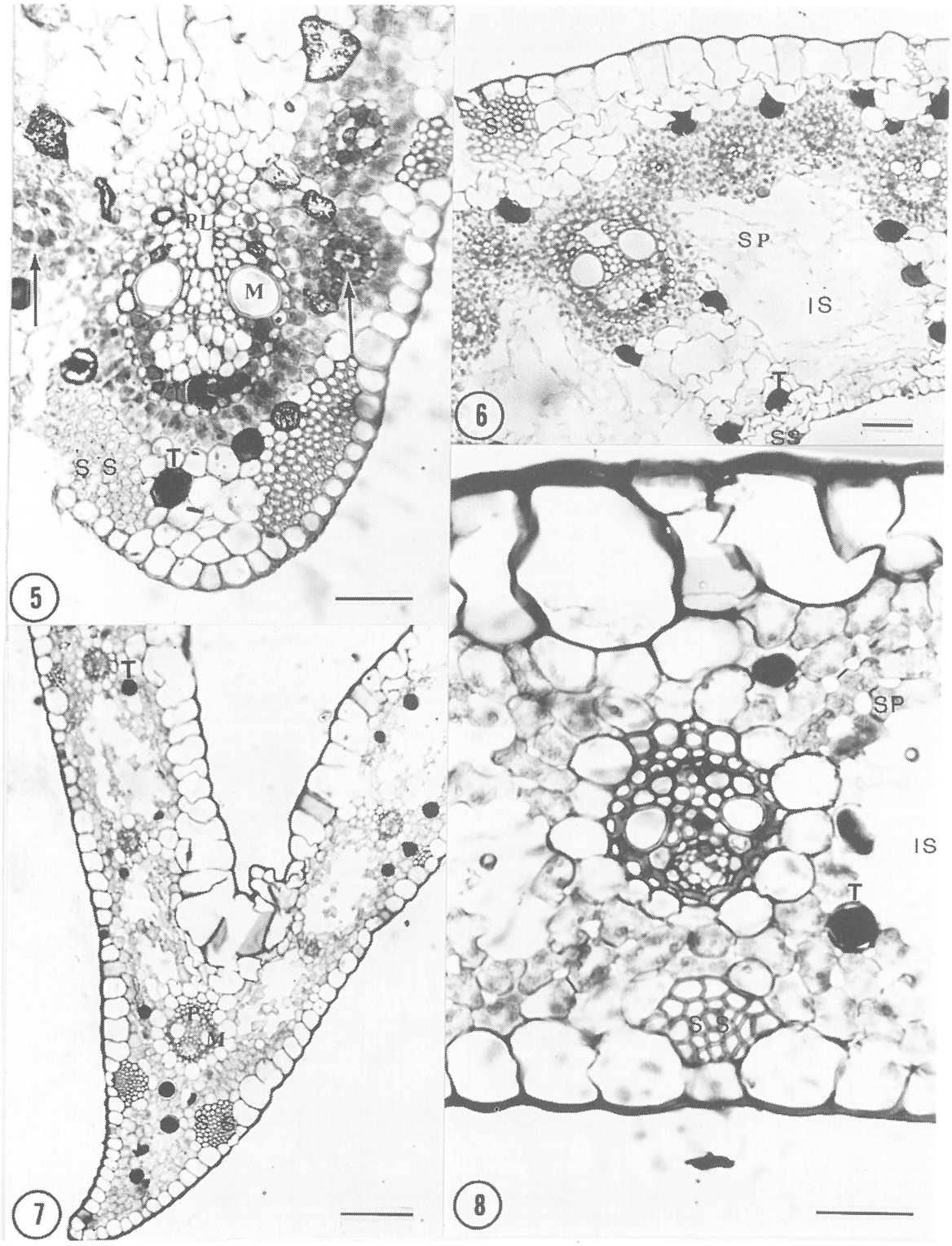

Figures 5, 6 Distributions of vascular bundles in the midrib (Figure 5) and the lamina (Figure 6) of *Cyperus fastigiatus*. **5.** An endodermoid sheath, comprising small lignified cells, separates PCA from PCR cells in the midrib bundle which contains large metaxylem vessels (M) and a protoxylem lacuna (PL). Hypodermal sclerenchymatous strands (SS) occur abaxially. Small vascular bundles (unlabelled arrows) contain an endodermoid sheath separating PCA from PCR cells. **6.** Portion of the lamina of *C. fastigiatus*. Note the large intercellular spaces (IS) and associated disintegrating stellate parenchyma (SP) cells. A large bundle is subtended by the mesophyll bridge formed between adjacent intercellular spaces. Translucent mesophyll cells occur beneath the intermediate bundle, which is associated with adaxial and abaxial hypodermal sclerenchymatous strands (SS). In both figures, numerous tannin cells (T) occur throughout the lamina. Scale bars: 10 μm.

Figures 7, 8 Distribution of vascular bundles in the midrib (Figure 7) and the lamina (Figure 8) of *Cyperus pulcher*. **7.** In contrast to *M. congestus*, *C. fastigiatus* and *C. albostriatus*, the inner tangential walls of the mestome sheath cells which separate the parenchymatous sheath from the vascular tissue, are noticeably thickened. The xylem consists of large metaxylem (M) and protoxylem (P). Sclerenchymatous hypodermal strands (SS) are located on either side of the large midrib bundle. **8.** Segment of the lamina of *C. pulcher*. Note the large intercellular spaces (IS) composed of stellate parenchyma (SP). In both figures, numerous tannin cells (T) occur throughout the lamina. Scale bars: 10 μm.

large vascular bundle which is associated with sclerenchymatous hypodermal strands abaxially (Figure 7). Vascular bundles within the leaf-blade are far apart and the vascular bundles are encircled by an essentially achloroplastic parenchymatous sheath (Figure 8). In this instance, both midrib and leaf-blade bundles are surrounded by a lignified mestome sheath layer.

Stomatal distribution

All four species have parasitic stomata. The distribution and density of the stomata of *C. albostriatus*, *C. fastigiatus*, *C. pulcher* and *M. congestus* are shown in Table 1. In *C. albostriatus* and *C. fastigiatus* the stomatal distribution is amphistomatous, whilst it is hypostomatous in *C. pulcher* and *M. congestus*.

Gas exchange characteristics

Light and temperature response

Examination of the light and temperature response curves for *C. albostriatus* (Figure 9), *C. fastigiatus* (Figure 10), *M. congestus* (Figure 11) and *C. pulcher* (Figure 12) indicates that *C. albostriatus* apparently light-saturates at 200 – 300 μmol m^{-2} s^{-1} between 20 and 35°C, whereas the highest assimilation rate was achieved by *M. congestus* (17.66 μmol m^{-2} s^{-1}) at 35°C (Figure 11). Like *M. congestus*, *C. fastigiatus* attained high photosynthetic rates at high temperature (15 μmol m^{-2} s^{-1} at 35°C, Figure 10). *C. pulcher*, on the other hand, was intermediate, with a low temperature optimum (20°C) and with a concomitantly lower photosynthetic rate (9.33 μmol m^{-2} s^{-1}, Figure 12). At 40°C, *M. congestus* was able to maintain an average of 10.2 μmol m^{-2} s^{-1} at light intensities above 1000 PPFD, whereas photosynthetic CO_2 gas exchange in *C. fastigiatus* hovered just above compensation point at all experimental light intensities. Clearly, *M. congestus* is the least temperature-sensitive of the four Cyperaceae examined in this study. Optimum photosynthetic temperatures determined for the four species are shown in Figure 13 and were as follows: *C. pulcher*, 20°C; *C. albostriatus*, 30°C; *C. fastigiatus* and *M. congestus*, 30 – 35°C.

Post-illumination CO_2 burst effect (PIB)

Upon removal of the light source, photosynthesis in *C. pulcher* declined from approximately 4 to –1.5 μmol m^{-2} s^{-1} within 30 s, rising slightly to –1.3 μmol m^{-2} s^{-1} for the duration of the PIB experiments. In contrast, both *M. congestus* and *C. albostriatus* continued to fix CO_2 at approximately the same pre-darkening rates (20.2 and 3.5 μmol m^{-2} s^{-1}, respectively) for two minutes, after which CO_2 fixation declined rapidly over the next two minutes, falling to steady-state respiration rates of –0.8 and –1.1 μmol m^{-2} s^{-1}, respectively. *C. fastigiatus*, on the other hand, demonstrated a measurable PIB effect. The pre-darkening CO_2 fixation rate was 6.5 μmol m^{-2} s^{-1} which rose within the first minute of the post-darkening period to 10.2 μmol m^{-2} s^{-1}, declining rapidly thereafter to –0.8 μmol m^{-2} s^{-1} two minutes after the commencement of the darkening phase. PIB effects are associated with either C_4-NAD-Me or C_4-PCK species (see Downton 1970), whilst the short, post-darkening steady-state CO_2 assimilation rate in *M. congestus* and *C. albo-*

Table 1 Stomatal densities for *C. albostriatus*, *C. fastigiatus*, *C. pulcher* and *M. congestus*

Species	Stomatal density / cm^2 leaf	
	Adaxial	Abaxial
Cyperus albostriatus	1147	1414
Cyperus fastigiatus	17	20
Cyperus pulcher	—	6000
Mariscus congestus	—	371

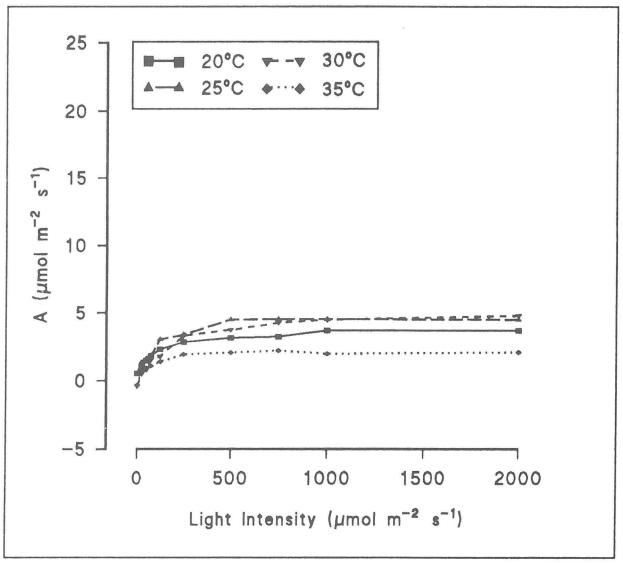

Figure 9 Light and temperature response of *Cyperus albostriatus*. This species appears to be light-saturated at approximately 500 μmol m^{-2} s^{-1}, which is atypical of C_4 photosynthesis. The data suggest that *C. albostriatus* has a low light requirement, with concomitant low CO_2 assimilation rates (4.6 μmol m^{-2} s^{-1}), even at its optimal photosynthetic temperature (30°C).

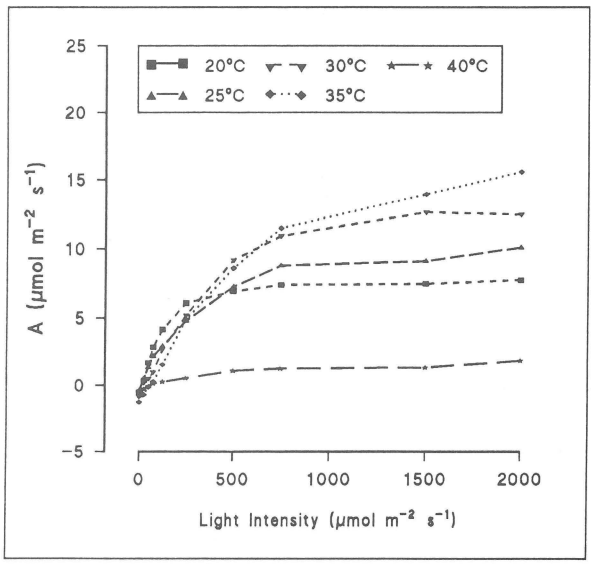

Figure 10 Light and temperature response of *Cyperus fastigiatus*. This species exhibits no apparent light saturation above 2000 μmol m^{-2} s^{-1}. Optimal photosynthetic temperature was 35°C. High photosynthetic rate at high temperature is indicative of C_4 photosynthesis.

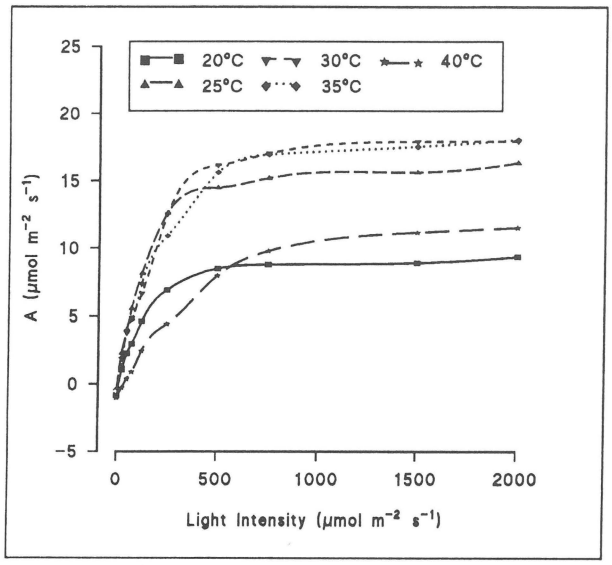

Figure 11 Light and temperature response of *Mariscus congestus*. Light-saturation was observed at its optimal photosynthetic temperature of between 30 and 35°C. *M. congestus* has the highest CO_2 assimilation rate of the species investigated (17.6 μmol m^{-2} s^{-1}).

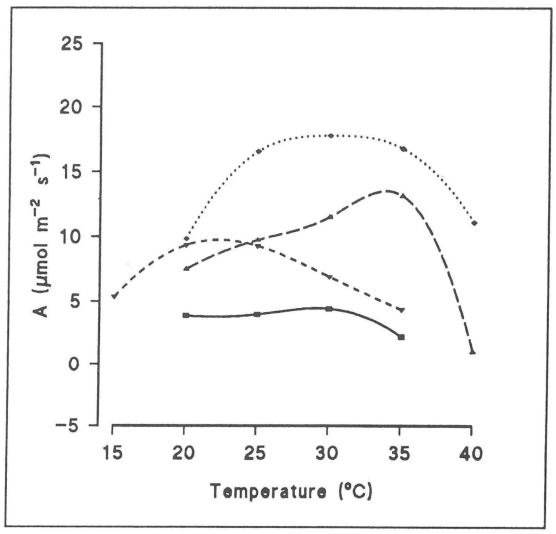

Figure 13 Temperature response curves of *M. congestus* (♦), *C. albostriatus* (■), *C. fastigiatus* (▲) and *C. pulcher* (▼) at 1500 μmol m^{-2} s^{-1} PPFD. *M. congestus attained the highest* A_{max} (17.6 μmol m^{-2} s^{-1}) at 30°C, *C. fastigiatus* (13.13 μmol m^{-2} s^{-1}) at 30 – 35°C, *C. pulcher* (9.3 μmol m^{-2} s^{-1}) at 20 – 25°C and *C. albostriatus* (4.6 μmol m^{-2} s^{-1}) at 30°C.

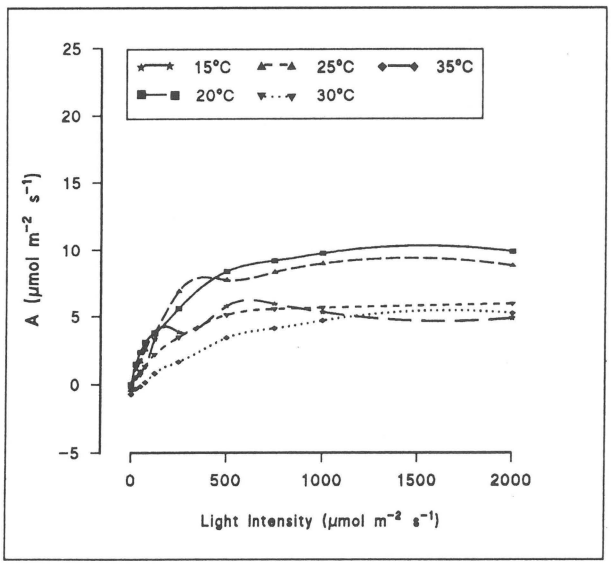

Figure 12 Light and temperature response in *Cyperus pulcher* which light-saturates at a light intensity approaching 1500 PPFD. Optimal photosynthetic temperature was 20°C, which is indicative of C_3 photosynthesis.

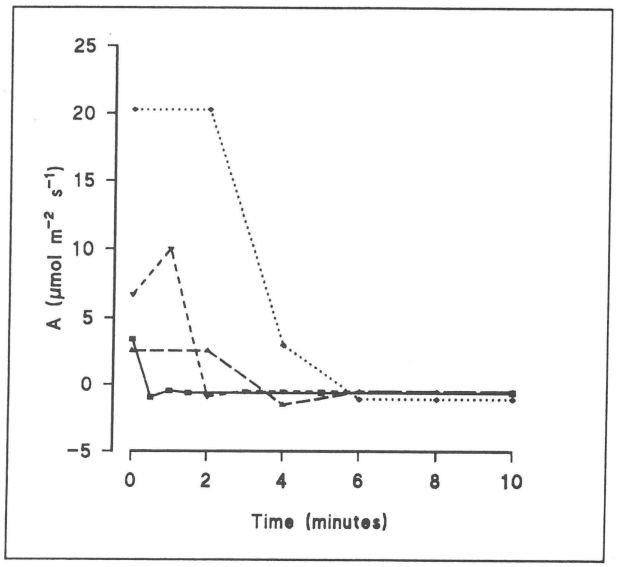

Figure 14 Post-illumination CO_2 burst effect in *C. fastigiatus* (▼), *C. pulcher* (■), *C. albostriatus* (▲) and *M. congestus* (♦). The only species that exhibited a clear post-illumination CO_2 burst was *C. fastigiatus*, indicating that it is a C_4 NAD-Me or PCK species.

striatus is indicative of C_4-NADP-Me photosynthesis (Figure 14.)

Discussion and Conclusions

Anatomical investigation confirmed that of the four species studied, three were C_4 (*C. albostriatus, C. fastigiatus* and *M. congestus*). These species had a maximum cell lateral count of four or less cells between vascular bundles (Hattersley & Watson 1975), which suggests that they are C_4 (Crookson & Moss 1974; Takeda *et al.* 1980; Monson *et al.* 1984). However, *C. pulcher* appears to be a C_3 species, as more than four mesophyll cells separate adjacent vascular bundles. The intermediate and small vascular bundles in the C_4 species examined are surrounded by Kranz mesophyll and a lignified (mestome) sheath which is characteristic of the chlorocyperoid *Cypereae* of the Cyperaceae (Chen *et al.* 1974; Brown 1975; Carolin *et al.* 1977; Hesla *et al.* 1982).

The optimal photosynthetic temperatures attained under the experimental conditions revealed that *C. albostriatus, C. fastigiatus* and *M. congestus* have optima above 30°C, which is indicative of C_4 species (Pearcy 1977; Teeri 1979; Doliner & Jolliffe 1979; Teeri *et al.* 1980; Berry & Björkman 1980). In contrast, *C. pulcher* has typical C_3 *Cypereae*, non-Kranz anatomy. *Cypereae* typically have a parenchymatous bundle sheath and internal to this, a

mestome sheath, surrounding the vascular tissue (Carolin *et al.* 1977; Hesla *et al.* 1982; Dengler *et al.* 1985; Ueno *et al.* 1988). Furthermore, this species had an optimal photosynthetic temperature, under experimental conditions, of below 30°C, which is, again, indicative of a C_3 photosynthetic pathway (Ehleringer & Björkman 1977; Teeri 1979; Teeri *et al.* 1980; Berry & Björkman 1980; Weis 1981; Monson *et al.* 1982).

Whilst the C_4 Cyperaceae have been widely reported to be NADP-Me species (Metcalfe 1969; Ueno *et al.* 1986), recent literature has shown that *Eleocharis vivipara, E. caespitasissima* and *E. retroflexan* are NAD-Me species (Bruhl *et al.* 1987; Ueno *et al.* 1988). The post-illumination burst effect experiments suggest that *M. congestus* and *C. albostriatus* may be NADP-Me, owing to their lack of discernible PIB effect. PIB effect observed in leaves of *C. fastigiatus* indicates that this species may be either a C_4 NAD-Me or PCK species, and aspartate former (Downton 1970, 1971).

Acknowledgements

The Foundation for Research Development and the Rhodes University Joint Research Committee are thanked for financial support.

References

BERRY, J. & BJÖRKMAN, O. 1980. Photosynthetic response and adaptation to temperatures in higher plants. *Ann. Rev. Pl. Physiol.* 31: 491 – 543.

BROWN, W.V. 1975. Variations in anatomy, associations, and origins of Kranz tissue. *Am. J. Bot.* 62: 395 – 402.

BRUHL, J.J., STONE, N.E. & HATTERSLEY, P.W. 1987. C_4 acid decarboxylation enzymes and anatomy in sedges (Cyperaceae): first record of NAD-Malic enzyme species. *Aust. J. Pl. Physiol.* 14: 719 – 728.

CAROLIN, R.C., JACOBS, S.W.L. & VESK, M. 1977. The ultrastructure of Kranz cells in the family Cyperaceae. *Bot. Gaz.* 138: 413 – 419.

CHEN, T.M., DITTRICH, P., CAMPBELL, W.H. & BLACK, C.C. 1974. Metabolism of epidermal tissues, mesophyll cells, and bundle sheath strands resolved from mature Nutsedge leaves. *Arch. Biochem. Biophys.* 163: 246 – 262.

CROOKSTON, R.K. & MOSS, D.N. 1974. Interveinal distances for carbohydrate transport in leaves of C_3 and C_4 grasses. *Crop Sci.* 14: 123 – 125.

DENGLER, N.G., DENGLER, R.E. & HATTERSLEY, P.W. 1985. Differing ontogenetic origins of PCR ('Kranz') sheaths in leaf blades of C_4 grasses (Poaceae). *Am. J. Bot.* 72: 284 – 302.

DOLINER, L.H. & JOLLIFFE, P.A. 1979. Ecological evidence concerning the adaptive significance of the C_4 dicarboxylic acid pathway of photosynthesis. *Oecologia* 38: 23 – 34.

DOWNTON, W.J.S. 1970. Preferential C_4-dicarboxylic acid synthesis, the postillumination CO_2 burst, carboxyl transfer step, and grana configurations in plants with C_4 photosynthesis. *Can. J. Bot.* 48: 1795 – 1800.

DOWNTON, W.J.S. 1971. Further evidence for two modes of carboxyl transfer in plants with C_4-photosynthesis. *Can. J. Bot.* 49: 1439 – 1442.

EHLERINGER, J. & BJÖRKMAN, O. 1977. Quantum yields for CO_2 uptake in C_3 and C_4 plants: dependence on temperature, CO_2 and O_2 concentrations. *Pl. Physiol.* 59: 86 – 90.

HATTERSLEY, P.W. & WATSON, L. 1975. Anatomical parameters for predicting photosynthetic pathways of grass leaves: The 'maximum lateral cell count' and the 'maximum cells distal count'. *Phytomorphology* 25: 325 – 333.

HESLA, B.I., TIESZEN, L.L. & IMBAMBA, S.K. 1982. A systematic survey of C_3 and C_4 photosynthesis in the Cyperaceae of Kenya, East Africa. *Photosynthetica* 16: 196 – 205.

JOHNSON, S.C. & BROWN, W.V. 1973. Grass leaf ultrastructure variations. *Am. J. Bot.* 60: 727 – 735.

LAETSCH, W.M. 1974. The C_4 syndrome: a structural analysis. *Ann. Rev. Pl. Physiol.* 25: 27 – 52.

METCALFE, C.R. 1969. Anatomy as an aid to classifying the Cyperaceae. *Am. J. Bot.* 56: 782 – 790.

MONSON, R.K., EDWARDS, G.E. & KU, M.S.B. 1984. C_3–C_4 intermediate photosynthesis in plants. *Bioscience* 34: 563 – 574.

MONSON, R.K., STIDHAM, M.A., WILLIAMS III, G.J. & EDWARDS, G.E. 1982. Temperature dependence of photosynthesis in *Agropyron smithii* Ryb. 1. Factors affecting net CO_2 uptake in intact leaves and contribution from ribulose 1,5-bisphosphate carboxylase/oxygenase measured *in vivo* and *in vitro*. *Pl. Physiol.* 69: 921 – 928.

PEARCY, R.W. 1977. Acclimation of photosynthetic and respiratory carbon dioxide exchange to growth temperature in *Atriplex lentiformis* (Torr.) Wats. *Pl. Physiol.* 59: 795 – 799.

PFEIFFER, H. 1927. Untersuchungen zur vergleichenden Anatomie der Cyperaceen. 1. Die Anatomie der Blätter. *Beihefte Bot. Centralbl.* 44: 90 – 176.

PLOWMAN, A.B. 1906. The comparative anatomy and phylogeny of the Cyperaceae. *Ann. Bot.* XX (LXXVII): 1 – 36.

RAYNAL, J. 1973. Notes Cyperologiques: 19. Contribution a la classification de la sous-famille des Cyperoideae. *Adansonia Ser.* 2: 145 – 171.

TAKEDA, T., UENO, O. & AGATA, W. 1980. The occurrence of C_4 species in the genus *Rhynchospora* and its significance in kranz anatomy of the Cyperaceae. *Bot. Mag. Tokyo* 93: 55 – 65.

TAKEDA, T., UENO, O., SAMEJIMA, M. & OHATANI, T. 1985. An investigation for the occurrence of C_4 photosynthesis in the Cyperaceae from Australia. *Bot. Mag. Tokyo* 98: 393 – 411.

TEERI, J.A. 1979. The climatology of the C_4 photosynthetic pathway. Topics in plant population biology. Columbia University Press, New York.

TEERI, J.A., STOWE, L.G. & LIVINGSTONE, D.A. 1980. The distribution of C_4 species of the Cyperaceae in North America in relation to climate. *Oecologia* 47: 307 – 310.

UENO, O., SAMEJIMA, M. & KOYAMA, T. 1989. Distribution and evolution of C_4 syndrome in *Eliocharis*, a sedge group inhabiting wet and aquatic environments, based on culm anatomy and carbon isotope ratios. *Ann. Bot.* 64: 425 – 438.

UENO, O., SAMEJIMA, M., MUTO, S. & MIYACHI, S. 1988. Photosynthetic characteristics of an amphibious plant, *Eleocharis vivipara*: Expression of C_4 and C_4 modes in contrasting environments. *Proc. Natl. Acad. Sci. U.S.A.* 85: 6733 – 6737.

UENO, O., TAKEDA, T. & MURATA, T. 1986. C_4 acid decarboxylating enzyme activitics of C_4 species possessing different kranz anatomical types in the Cyperaceae. *Photosynthetica* 20: 111 – 116.

WEIS, E. 1981. Reversible heat-inactivation of the Calvin cycle: A possible mechanism of the temperature regulation of photosynthesis. *Planta* 151: 33 – 39.